# Isotopic Scaling and the Symmetry Energy in Spectator Fragmentation

A. Le Fèvre,[1] G. Auger,[2] M. L. Begemann-Blaich,[1] N. Bellaize,[3] R. Bittiger,[1] F. Bocage,[3] B. Borderie,[4] R. Bougault,[3] B. Bouriquet,[2] J. L. Charvet,[5] A. Chbihi,[2] R. Dayras,[5] D. Durand,[3] J. D. Frankland,[2] E. Galichet,[6,11] D. Gourio,[1] D. Guinet,[6] S. Hudan,[2] G. Immé,[7] P. Lautesse,[6] F. Lavaud,[4] R. Legrain,[5,*] O. Lopez,[3] J. Łukasik,[1,12] U. Lynen,[1] W. F. J. Müller,[1] L. Nalpas,[5] H. Orth,[1] E. Plagnol,[4] G. Raciti,[7] E. Rosato,[8] A. Saija,[7] C. Schwarz,[1] W. Seidel,[9] C. Sfienti,[1] B. Tamain,[3] W. Trautmann,[1] A. Trzciński,[10] K. Turzó,[1] E. Vient,[3] M. Vigilante,[8] C. Volant,[5] B. Zwiegliński,[10] and A. S. Botvina[1,13]

(INDRA and ALADIN Collaborations)

[1]*Gesellschaft für Schwerionenforschung mbH, D-64291 Darmstadt, Germany*
[2]*GANIL, CEA et IN2P3-CNRS, F-14076 Caen, France*
[3]*LPC, IN2P3-CNRS, ISMRA et Université, F-14050 Caen, France*
[4]*Institut de Physique Nucléaire, IN2P3-CNRS et Université, F-91406 Orsay, France*
[5]*DAPNIA/SPhN, CEA/Saclay, F-91191 Gif sur Yvette, France*
[6]*Institut de Physique Nucléaire, IN2P3-CNRS et Université, F-69622 Villeurbanne, France*
[7]*Dipartimento di Fisica dell' Università and INFN, I-95129 Catania, Italy*
[8]*Dipartimento di Scienze Fisiche e Sezione INFN, Università Federico II, I-80126 Napoli, Italy*
[9]*Forschungszentrum Rossendorf, D-01314 Dresden, Germany*
[10]*A. Sołtan Institute for Nuclear Studies, Pl-00681 Warsaw, Poland*
[11]*Conservatoire National des Arts et Métiers, F-75141 Paris Cedex 03, France*
[12]*H. Niewodniczański Institute of Nuclear Physics, Pl-31342 Kraków, Poland*
[13]*Institute for Nuclear Research, 117312 Moscow, Russia*
(Received 20 September 2004; published 26 April 2005)

Isotopic effects in the fragmentation of excited target residues following collisions of $^{12}$C on $^{112,124}$Sn at incident energies of 300 and 600 MeV per nucleon were studied with the INDRA $4\pi$ detector. The measured yield ratios for light particles and fragments with atomic number $Z \leq 5$ obey the exponential law of isotopic scaling. The deduced scaling parameters decrease strongly with increasing centrality to values smaller than 50% of those obtained for the peripheral event groups. Symmetry-term coefficients, deduced from these data within the statistical description of isotopic scaling, are near $\gamma = 25$ MeV for peripheral and $\gamma < 15$ MeV for central collisions.

DOI: 10.1103/PhysRevLett.94.162701 PACS numbers: 25.70.Mn, 24.10.Pa, 25.70.Pq

The growing interest in isospin effects in nuclear reactions is motivated by an increasing awareness of the importance of the symmetry term in the nuclear equation of state, in particular, for astrophysical applications. Supernova simulations or neutron star models require inputs for the nuclear equation of state at extreme values of density and asymmetry [1–3]. The demonstration in the laboratory of the effects of the symmetry term at abnormal densities is, therefore, an essential first step within a program aiming at gaining such information experimentally [4,5].

Multifragmentation is generally considered a low-density phenomenon, with a high degree of thermalization believed to be reached. Accepting the concept of a freeze-out volume and the applicability of grand-canonical logic, the probability of producing a cluster of a given atomic number $Z$ and mass $A$ at temperature $T$ depends exponentially on the free energy of that cluster, $F(Z, A, T)$. The cluster free energies depend on the strength of the symmetry term $E_{\mathrm{sym}} = \gamma(A - 2Z)^2/A$ in the liquid-drop energy which, in turn, must depend on the extent of expansion of the fragments. This work makes use of an observable that isolates the symmetry contribution to the cluster free energy to explore the difference in this term for fragments produced in peripheral and central collisions. It is found that, while the sequential decay strongly degrades the quality of this observable, the symmetry energy coefficient does indeed decrease as the collisions producing the fragments become more violent.

In the Copenhagen statistical multifragmentation model (SMM), standard coefficients $\gamma = 23$ to 25 MeV are used to describe the nascent fragments [6–8]. In the freeze-out scenario adopted there, normal-density fragments are considered to be statistically distributed within an expanded volume, and the density is only low on average. An experimental value for $\gamma$ of about standard magnitude has recently been obtained within a statistical description of isotopic scaling in light-ion ($p$, $d$, $\alpha$) induced reactions at relativistic energies of up to 15 GeV [7]. This result, however, may not be representative for multifragment

 

decays because the data were inclusive and the mean multiplicities of intermediate-mass fragments correspondingly small [9]. In the present work, we apply the same method to exclusive data obtained with heavier projectiles, $^{12}$C on $^{112}$Sn and $^{124}$Sn targets at 300 and 600 MeV per nucleon incident energy. Here, according to the established systematics [10], maximum fragment production occurs at central impact parameters.

Isotopic scaling, also termed isoscaling, has been shown to be a phenomenon common to many different types of heavy-ion reactions [7,11–13]. It is observed by comparing product yields from otherwise identical reactions with isotopically different projectiles or targets, and it is constituted by an exponential dependence of the measured yield ratios $R_{21}(N, Z)$ on the neutron number $N$ and proton number $Z$ of the considered product. The scaling expression

$$R_{21}(N, Z) = Y_2(N, Z)/Y_1(N, Z) = C \exp(\alpha N + \beta Z) \quad (1)$$

describes rather well the measured ratios over a wide range of complex particles and light fragments [14].

In the grand-canonical approximation, assuming that the temperature $T$ is about the same, the scaling parameters $\alpha$ and $\beta$ are proportional to the differences of the neutron and proton chemical potentials for the two systems, $\alpha = \Delta\mu_n/T$ and $\beta = \Delta\mu_p/T$. Of particular interest is their connection with the symmetry-term coefficient. It has been obtained from the statistical interpretation of isoscaling within the SMM [7] and expanding-emitting-source model [14] and confirmed by an analysis of reaction dynamics [15]. The relation is

$$\alpha T = \Delta\mu_n = \mu_{n,2} - \mu_{n,1} \approx 4\gamma\left(\frac{Z_1^2}{A_1^2} - \frac{Z_2^2}{A_2^2}\right) \quad (2)$$

where $Z_i$ and $A_i$ are the charges and mass numbers of the two systems (the indices 1 and 2 denote the neutron poor and neutron rich system, respectively). With the knowledge of the temperature and the isotopic compositions, the coefficient $\gamma$ of the symmetry term can be obtained from isoscaling.

The data were obtained with the INDRA multidetector [16] in experiments performed at the GSI. Beams of $^{12}$C with 300 and 600 MeV per nucleon incident energy, delivered by the heavy-ion synchrotron SIS, were directed onto enriched targets of $^{112}$Sn (98.9%) and $^{124}$Sn (99.9%) with areal densities between 1.0 and 1.2 mg/cm$^2$. Light charged particles and fragments ($Z \leq 5$) were detected and isotopically identified with the calibration telescopes of rings 10 to 17 of the INDRA detector, which cover the range of polar angles $45° \leq \theta_{lab} \leq 176°$. These telescopes consist of pairs of an 80-$\mu$m Si detector and a 2-mm Si(Li) detector which are mounted between the ionization chamber and the CsI(Tl) crystal of one of the modules of a ring [16]. Further experimental details may be found in [17] and the references given therein. For impact-parameter selection, the charged-particle multiplicity $M_C$ measured with the full detector was used, and four bins were chosen for the sorting of the data. For 600 MeV per nucleon, the two most central bins were combined for reasons of counting statistics.

Kinetic energy spectra of light reaction products with $Z \leq 5$, integrated over the impact parameter and the angular range $\theta_{lab} \geq 45°$, are shown in Fig. 1. To reduce preequilibrium contributions, upper limits of 20 and 70 MeV were set for hydrogen and helium isotopes, respectively, which, however, are not crucial. The spectra of Li, Be, and B fragments were integrated above the energy thresholds for isotopic identification which amounted to 28, 40, and 52 MeV, respectively.

The ratios of the fragment yields measured for the two reactions and integrated over the chosen intervals of energy and angle ( $\theta_{lab} \geq 45°$) obey the law of isoscaling. This is illustrated in Fig. 2, which shows the scaled isotopic ratios $S(N) = R_{21}(N, Z)/\exp(\beta Z)$. Their slope parameters change considerably with impact parameter, extending from $\alpha = 0.62$ to values as low as $\alpha = 0.25$ for the most central event group at 600 MeV per nucleon (Table I and Fig. 3, top).

Temperature estimates were obtained from the yields of $^{3,4}$He and $^{6,7}$Li isotopes, and the deduced $T_{HeLi}$ contains a correction factor of 1.2 for the effects of sequential decay [18,19]. The temperatures are quite similar for the two target cases and increase with centrality from about 6 to

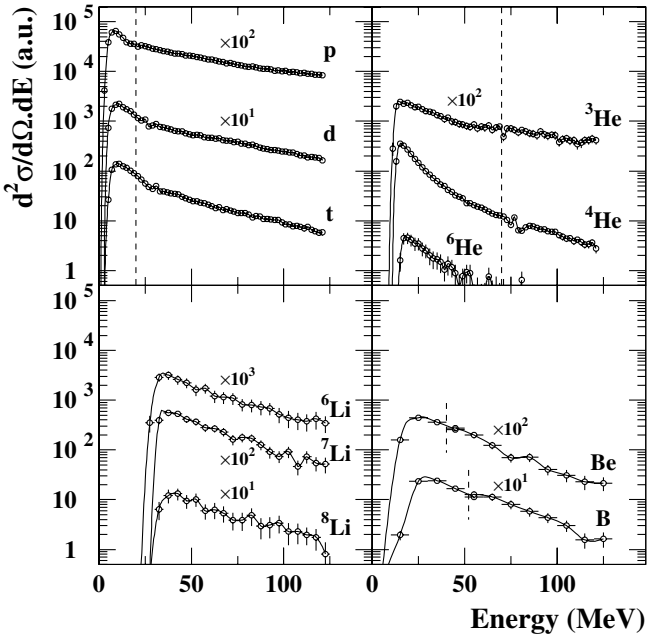


FIG. 1. Energy spectra of H, He, and Li isotopes, and of Be and B elements, measured with the calibration telescopes for $^{12}$C + $^{124}$Sn at 300 MeV per nucleon. The dashed lines indicate the upper limits set for $Z = 1$, 2 in the analysis and the identification thresholds for $Z = 4$, 5.

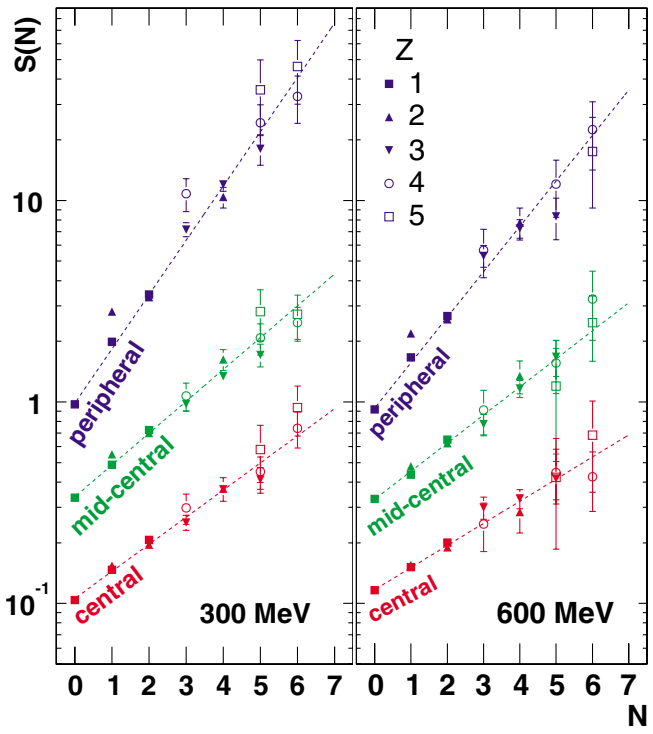


FIG. 2 (color online). Scaled isotopic ratios $S(N)$ for $^{12}C + ^{112,124}Sn$ at $E/A = 300$ MeV (left panel) and 600 MeV (right panel) for the intervals of reduced impact parameter specified in Table I, with "central" indicating $b/b_{max} \leq 0.4$ and with offset factors of multiples of three. The dashed lines are the results of exponential fits according to Eq. (1). Only statistical errors are displayed.

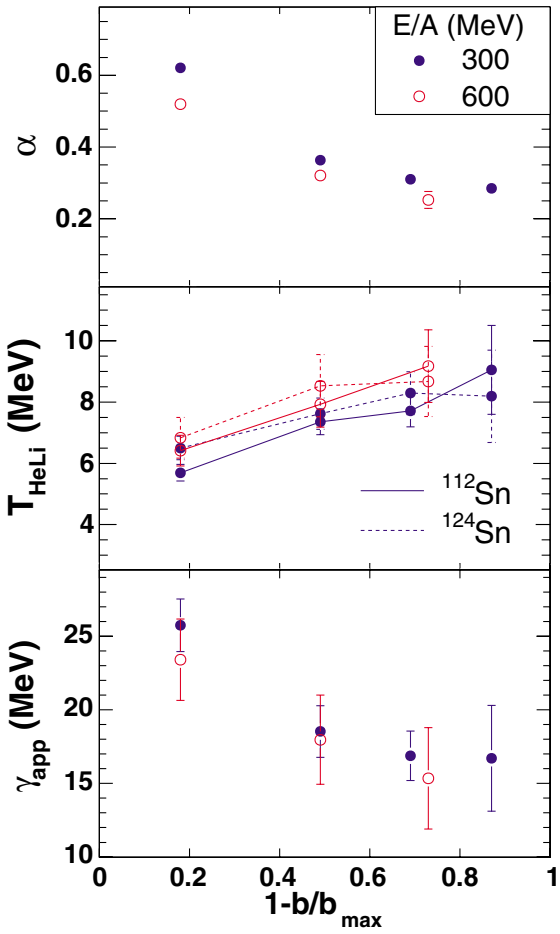


FIG. 3 (color online). Isoscaling coefficient $\alpha$ (top), double-isotope temperatures $T_{HeLi}$ (middle), and resulting $\gamma_{app}$ (bottom) for $E/A = 300$ MeV (filled symbols) and 600 MeV (open symbols), as a function of the centrality parameter $1 - b/b_{max}$. The temperatures for the $^{112}Sn$ and $^{124}Sn$ targets are distinguished by solid and dashed lines, respectively.

9 MeV (Fig. 3, middle). This is consistent with the results obtained for $^{197}Au$ fragmentations [18,19] and with the established dependence on the system mass [20]. The rise of $T_{HeLi}$, however, does not compensate for the decrease of $\alpha$, as it did in the case of light-particle induced reactions [7], and $\Delta\mu_n$, consequently, decreases toward the central collisions.

The analytical expression for $\Delta\mu_n$ [Eq. (2)] contains the isotopic compositions of the sources, more precisely the difference of the squared $Z/A$ values, $\Delta(Z^2/A^2) = (Z_1/A_1)^2 - (Z_2/A_2)^2$. For the target spectators, this quantity is not expected to deviate significantly from its original value [7], in contrast to mean-field dominated reaction systems at intermediate energies [15,21]. This was confirmed with calculations performed with the Liège-cascade-percolation model [22] and with the relativistic mean-field model [relativistic Boltzmann-Uehling-Uhlenbeck (RBUU), Ref. [23]] in which isotopic effects of the nuclear mean field are treated explicitly. The individual $Z/A$ values change slightly but $\Delta(Z^2/A^2)$ remains nearly the same. For central collisions at 600 MeV per nucleon, e.g., the RBUU calculations predict a reduction of $\Delta(Z^2/A^2)$ by 6% for the target-rapidity region after 90 fm/c collision time.

TABLE I. Parameters obtained from fitting the measured isotopic yield ratios with the scaling function given in Eq. (1).

| | 300 MeV | | 600 MeV | |
|---|---|---|---|---|
| $b/b_{max}$ | $\alpha$ | $\beta$ | $\alpha$ | $\beta$ |
| 0.0 - 0.2 | $0.28 \pm 0.01$ | $-0.33 \pm 0.03$ | | |
| 0.2 - 0.4 | $0.31 \pm 0.01$ | $-0.32 \pm 0.01$ | $0.25 \pm 0.02$ | $-0.28 \pm 0.04$ |
| 0.4 - 0.6 | $0.36 \pm 0.01$ | $-0.39 \pm 0.02$ | $0.32 \pm 0.02$ | $-0.34 \pm 0.03$ |
| 0.6 - 1.0 | $0.62 \pm 0.01$ | $-0.68 \pm 0.02$ | $0.52 \pm 0.02$ | $-0.59 \pm 0.03$ |

The suggested corrections are small and can thus be temporarily ignored. With the compositions of the original targets, $\Delta(Z^2/A^2) = 0.0367$, the expression $\gamma = \alpha T/0.147$ is obtained from Eq. (2). It was used to determine an apparent symmetry-term coefficient $\gamma_{app}$, i.e., without sequential decay corrections for $\alpha$, from the data shown in Fig. 3 (the mean values were used for $T$). The

results are close to the normal-density coefficient for peripheral collisions but drop to lower values at the more central impact parameters (Fig. 3, bottom).

The effects of sequential decay were studied with the microcanonical Markov-chain version of the statistical multifragmentation model [24]. The target nuclei $^{112,124}$Sn with excitation energies of 4, 6, and 8 MeV per nucleon were chosen as inputs, and the symmetry term $\gamma$ was varied between 4 and 25 MeV. The isoscaling coefficient $\alpha$ was determined from the calculated fragment yields before (hot fragments) and after (cold fragments) the sequential decay stage of the calculations for which standard values for the fragment masses were used. The energy balance at freeze-out and during the secondary deexcitation was taken into account as described in [6].

The hot fragments exhibit the linear relation of $\alpha$ with $\gamma$ as expected (Fig. 4, top panel). With $\gamma = 25$ MeV, the sequential processes cause a slight broadening of the isotopic distributions and the resulting $\alpha$ is lowered by 10% to 20%, similar to what was reported in [7]. For smaller values of $\gamma$, however, larger changes of $\alpha$ are predicted. The decay of the wings of the wider distributions of hot fragments toward the valley of stability causes the resulting cold distributions to be narrower and the isoscaling coefficients to be larger. The overall variation of $\alpha$ with $\gamma$ is weaker, and the decrease of $\gamma$ with centrality should, thus, be stronger than that of $\gamma_{\mathrm{app}}$ (Fig. 3). For central collisions, this implies $\gamma < 15$ MeV as an upper limit but much smaller values are more likely to be expected. With the present calculations, for excitation energies up to 8 MeV per nucleon and the original target compositions, the measured $\alpha < 0.3$ is only reproduced with $\gamma \approx 6$ MeV (Fig. 4, top).

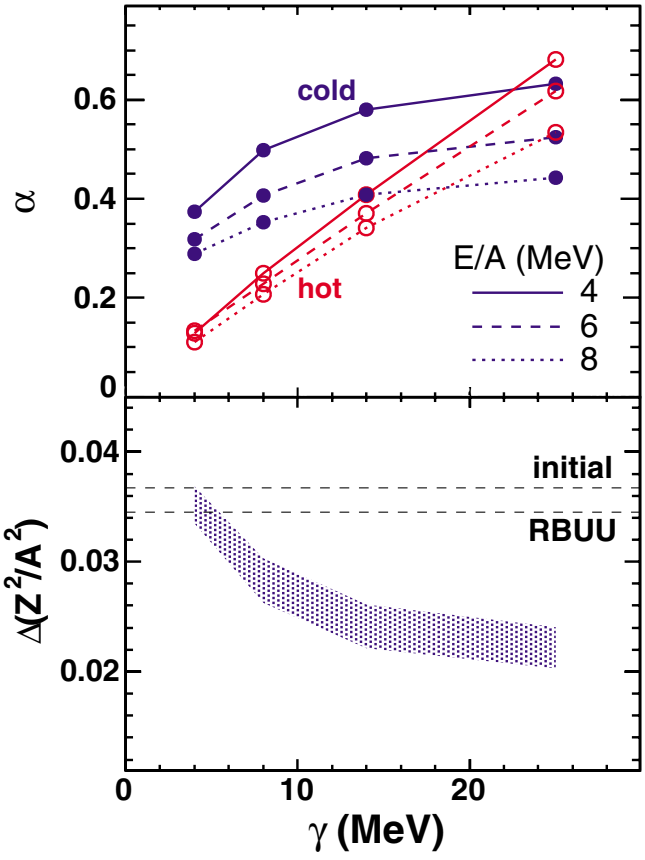


FIG. 4 (color online). Top panel: isoscaling coefficient $\alpha$ for hot (open circles) and cold fragments (dots) as a function of the symmetry-term coefficient $\gamma$ as predicted by the Markov-chain calculations for $^{112,124}$Sn. Bottom panel: region in the $\Delta(Z^2/A^2)$-versus-$\gamma$ plane consistent with the measured value $\alpha = 0.29$ for central collisions and with the Markov-chain predictions for cold fragments (shaded area). The dashed lines indicate the $\Delta(Z^2/A^2) = 0.0367$ of $^{112,124}$Sn and the RBUU prediction.

The bottom panel of Fig. 4 shows how the situation changes when the variation of the isotopic compositions of the two systems is again included as a degree of freedom. The shaded band in the plane of $\Delta(Z^2/A^2)$ versus $\gamma$ represents the region consistent with the weighted mean $\alpha = 0.29$ measured for the central bins ($b/b_{\mathrm{max}} \leq 0.4$) at the two energies. It was obtained from the predictions $\alpha(\gamma)$ for cold fragments at excitation energies between 6 and 8 MeV per nucleon (Fig. 4, top) according to $\Delta(Z^2/A^2) = 0.0367 \cdot 0.29/\alpha(\gamma)$, i.e., using that $\alpha$ is, to first order, proportional to the difference of the isotopic compositions, here expressed by $\Delta(Z^2/A^2)$ (see, e.g., [7,15]). If this difference remains close to the cascade and RBUU predictions the resulting symmetry-term coefficient for the central reaction channels is very small, $\gamma \leq 10$ MeV. To restore the compatibility with a standard $\gamma \approx 25$ MeV would require considerable isotopic asymmetries in the initial reaction phase, much larger than what is expected according to the models.

In conclusion, the observed decrease of the isoscaling parameter $\alpha$ with centrality which is not compensated by a correspondingly increasing temperature requires a decreasing symmetry-term coefficient $\gamma$ in a statistical description of the fragmentation process. The effect is enhanced if sequential fragment decay is taken into account. Values less than 15 MeV, as obtained from the present analysis, are not necessarily unreasonable in a realistic description of the chemical freeze-out state. Besides the global expansion of the system also the possibly expanded or deformed structure of the forming fragments as well as their interaction with other fragments and with the surrounding nucleon gas will have to be considered. The presented results depend, crucially, on the isotopic evolution of the multifragmenting system as it approaches the chemical freeze-out and, more quantitatively, on the treatment of sequential decay in the analysis. These questions deserve further attention.

The authors would like to thank T. Gaitanos for communicating the results of RBUU calculations and for valuable discussions. This work was supported by the European

Community under contract ERBFMGECT950083.

*Deceased.

[1] J. M. Lattimer *et al.*, Phys. Rev. Lett. **66**, 2701 (1991).
[2] J. M. Lattimer and M. Prakash, Phys. Rep. **333**, 121 (2000).
[3] A. S. Botvina and I. N. Mishustin, Phys. Lett. B **584**, 233 (2004).
[4] Bao-An Li, Phys. Rev. Lett. **88**, 192701 (2002).
[5] V. Greco *et al.*, Phys. Lett. B **562**, 215 (2003).
[6] J. P. Bondorf *et al.*, Phys. Rep. **257**, 133 (1995).
[7] A. S. Botvina, O. V. Lozhkin, and W. Trautmann, Phys. Rev. C **65**, 044610 (2002).
[8] The notation follows that originally chosen in Ref. [6]; alternatively $C_{\mathrm{sym}}$ is frequently used for the same quantity.
[9] L. Beaulieu *et al.*, Phys. Lett. B **463**, 159 (1999) and Phys. Rev. Lett. **84**, 5971 (2000).
[10] A. Schüttauf *et al.*, Nucl. Phys. **A607**, 457 (1996).
[11] M. B. Tsang *et al.*, Phys. Rev. Lett. **86**, 5023 (2001).
[12] G. A. Souliotis *et al.*, Phys. Rev. C **68**, 024605 (2003).
[13] W. A. Friedman, Phys. Rev. C **69**, 031601(R) (2004).
[14] M. B. Tsang *et al.*, Phys. Rev. C **64**, 054615 (2001).
[15] A. Ono *et al.*, Phys. Rev. C **68**, 051601(R) (2003).
[16] J. Pouthas *et al.*, Nucl. Instrum. Methods Phys. Res., Sect. A **357**, 418 (1995).
[17] K. Turzó *et al.*, Eur. Phys. J. A **21**, 293 (2004).
[18] J. Pochodzalla *et al.*, Phys. Rev. Lett. **75**, 1040 (1995).
[19] Hongfei Xi *et al.*, Z. Phys. A **359**, 397 (1997); Eur. Phys. J. A **1**, 235 (1998).
[20] J. B. Natowitz *et al.*, Phys. Rev. C **65**, 034618 (2002).
[21] D. V. Shetty *et al.*, Phys. Rev. C **70**, 011601(R) (2004).
[22] C. Volant *et al.*, Nucl. Phys. **A734**, 545 (2004).
[23] T. Gaitanos *et al.*, Nucl. Phys. **A732**, 24 (2004), and (private communication).
[24] A. S. Botvina and I. N. Mishustin, Phys. Rev. C **63**, 061601(R) (2001).